ISTITUTO NAZIONALE DI FISICA NUCLEARE

Sezione di Genova

INFN/BE-95/01
15 Febbraio 1995

F. Gatti, G. Morelli, G. Testera, S. Vitale:

LIQUID SCINTILLATORS FOR LARGE MASS AND LOW BACKGROUND DETECTORS

SIS-Pubblicazioni
dei Laboratori Nazionali di Frascati

INFN – Istituto Nazionale di Fisica Nucleare
Sezione di Genova

INFN/BE–95/01
15 Febbraio 1995

LIQUID SCINTILLATORS FOR LARGE MASS AND LOW BACKGROUND DETECTORS

F. Gatti, G. Morelli, G. Testera, S. Vitale

Abstract

The attenuation length of liquid scintillator mixtures suitable for large scale and low background experiments like BOREXINO is measured. Attenuation lengths of the order of some metres have been obtained by a careful control of the purity and cleanliness of the components. The possible contribution of processes of radiative transport is discussed.

1.INTRODUCTION

This paper describes the results of a set of mesurements performed to investigate the optical properties of a liquid scintillator mixture suitable for the Borexino detector [1] and its small scale prototype called the Counting Test Facility (CTF)[2]. Borexino is one of the new detectors that should contribute in solving the well known "solar neutrino problem" [3], that is, the discrepancy between the measured solar neutrino flux and the predicted one. The solution of this puzzle is one of the most important aim of contemporary physics and it has implications both in fundamental physics and in astrophysics. Different experimental apparatus have already detected solar neutrinos [4],[5],[6],[7] and others are in construction with the goal of detecting neutrinos of different flavours and sampling the solar neutrino energy spectrum in different regions [1],[8],[9],[10], [11]. Borexino is a detector for neutrinos of any flavour with energy above 0.4 MeV and is designed for the observation of the monoenergetic neutrinos coming from the decay of ^7Be in the sun. The apparatus will be mounted underground in the Laboratori Nazionali del Gran Sasso (Italy). The detector will consist of a 8.5 m diameter spherical vessel filled by a 300 tons of liquid scintillator and viewed by approximately 2000 photomultipliers. All this equipment will be placed inside a cylindrical tank (16.5 m height and 16.5 m diameter) filled with 3500 tons of ultrapure water which shields the apparatus from the gamma rays coming from the rock.

The main reaction allowing the neutrino detection will be neutrino-electron elastic scattering which gives, for the ^7Be neutrinos, a flat distribution of events with an energy realease in the range $0 - 650$ keV. In this low energy range, natural radioactivity is one of the main contributions to the background which could mimic the neutrino signal. Particular care must be devoted to the choice and the preocessing

of all the materials used to construct the detector and an important factor is the choice and the handling of the liquid scintillator. The CTF has been built in Gran Sasso to measure and experimentally understand the background signal that will be associated with the Borexino detector. CTF resembles a small scale Borexino: it consists of 100 photomultipliers which detect the light emitted by 4 tons of liquid scintillator placed inside a nylon bag of 2 metres diameter. The photomultipliers and the scintillator bag are mounted inside a cylindrical tank (10 metres high and 11 metres diameter) filled with ultrapure water.

Both in CTF and in Borexino the charge of the photomultiplier signals and the time difference of the PMT signals will be measured for every event. The charge measurement the energy deposited inside the scintillator to be determined and timing of photons permits one to localize the scintillation and to define a fiducial volume with a buffer region in the scintillator which serves as final shielding. It is clear that the performances of both CTF and Borexino are determined by the scintillator optical properties. The ideal scintillator would have:

- a maximal optical yield and an attenuation length as long as possible to allow the detection of low energy signals;

- a time response as fast as possible, to allow a good spatial resolution;

- a composition as simple as possible to allow continuous distillation and purification during the run of the apparatus. In fact the scintillator is subject to radioactive purity requirements more stringent than any previously demonstrated values. The required content of Uranium and Thorium in the scintillator has to be at a level of 10^{-16} g/g and this can be reached and mantained only with sophisticated distillation and purification processes [1];

- low cost and low toxicity.

The choice of the optimum scintillator for Borexino and CTF is a compromise of the above conditions. The purpose of the measurements, described here, is to characterize some scintillator mixtures, in particular regarding the attenuation length.

2. DESCRIPTION OF THE APPARATUS

A test counter has been built to measure the scintillator self-absorption properties in conditions very similar to that of CTF and Borexino, that is:

- with a light path of the order of some metres;
- with signals corresponding to few (less than 10) photoelectrons detected for every event.

The apparatus is shown in Fig. 1. The liquid scintillator is contained in a cylindrical Pyrex cell 2 m long and 8 cm in diameter with flat end-faces. The thickness of the cell wall is 2 mm. The cell is contained in a 40 cm diameter and 3 m long PVC tube which is light tight and has a photomultiplier at each end. In the following we will refer to them as PMT1 and PMT2. The inside wall of the PVC tube and the outer wall of the Pyrex cell are painted black. A black disk, mounted at each end of the Pyrex cell, ensures that each PMT collects only the light emerging from the Pyrex cell flat end faces. We have chosen the same type of photomultipliers that are used in CTF that is the EMI 9351KA (with 12 dynodes and a spherical photocathode having an area of about 300 cm^2)

Fig. 2 shows the response of our apparatus as a function of the light wavelength: it is the superposition of the quantum efficiency of the photomultiplers (as released by the EMI company) and the transmittance of the Pyrex window. The absorbance of our Pyrex window has been carefully measured as a function of the wavelength; the data show that the flat end faces of the Pyrex tube transmit a fraction $A_{Py} = 0.97 \pm$

0.01 of the incident light when the wavelength exceeds about 340 nm. For smaller wavelength values both the transparency and the quantum efficiency decrease. By taking into account that the mixtures investigated have emission spectra starting from about 350 nm [12],[13], the Pyrex window does not distort in appreciable way the wavelength spectrum of the detected light.

A Cs^{137} (10 μCurie) γ ray source (E_γ = 660 keV) is used to illuminate the scintillator. The source is placed in a lead collimator and this gives rise to a γ ray beam having a longitudinal spread σ=1.2 cm (Fig.3). The dominant interaction process undergone by the γ rays is Compton scattering. A NaI counter, placed outside the PVC tube (see fig. 3), allows the detection of the backscattered $\gamma's$ at an angle of $150^o \pm 15^o$. The data acquisition system is triggered by the coincidence among the signal of PMT1, the signal of PMT2 and the signal coming from the NaI counter: the events selected in this way correspond to a rather well defined energy deposit E inside the scintillator

$$E = 464 \pm 10 \quad keV \tag{1}$$

By moving the assembly of the source with its lead collimator and the NaI counter along a direction parallel to the axis of the cell, scintillation events can be generated in different longitudinal position and the self-absorption of the scintillator can be investigated. Moreover, since we know the energy deposit of the selected events, the number of photoelectrons detected by a EMI PMT, when the source is near one end of the Pyrex cell, allows one to estimate the yield of the scintillator.

2.1 Optical properties

The Compton scattered electrons produce well localized scintillation events with photons uniformly emitted over the solid angle. Depending on the polar angle θ_{sci}

(see Fig. 4), the emitted light will either be totally reflected at the interface between the scintillator and the Pyrex cell or it will be absorbed by the dark external wall of the Pyrex cell.

Some measurements were performed with the Pyrex cell centered in the apparatus and others with the cell shifted to the left toward PMT1 in order to maximize the signal. The final results are independent of the geometrical configuration and in the following we will refer to a geometrical setup where PMT1 is at 45 cm from the Pyrex cell and the distance between PMT2 and the right end of the cell is 63 cm. In any case, the distances between the two PMTs and the flat end of the glass tube were chosen in order i) to collect the photons which travelled only within the scintillator and ii) to select the light emitted with a small angle θ_{sci}. This allows to have a negligeable spread in the pathlength of photons originating in the same point.

For reference, let us consider a scintillation event producing a photon emerging in the center of the flat end of the Pyrex cell (fig. 4). Let us call θ_{air} the angle with respect to the system axis when the photon propagates in air from the exit window of the Pyrex tube to PMT1. The photon will be collected by PMT1 only if

$$\theta_{air} < atan(\frac{r}{D_1}) \tag{2}$$

where r =10 cm is the radius of the PMT photocathode and D_1 = 45 cm is the PMT1-pyrex tube distance. The corresponding θ_{sci} angle inside the scintillator is related to θ_{air} by the well known refraction law across the interfaces scintillator-pyrex and pyrex-air; using the refractive index of the scintillator $n_{sci} = 1.505$ and $n_{air} = 1$ for the air, we see that the collected light is emitted inside the scintillator with an angle θ_{sci}

$$\theta_{sci} < 8.3^o \tag{3}$$

In this simple situation the two conditions i) and ii) are satisfied. In fact, using the maximum θ_{sci} angle, we get the result that the pathlength of the collected photons differs from z (axial coordinate of the source position) only by $1-1/cos(8.3^o) \simeq 0.01$ and, using the value $n_{Py} = 1.472$ for the Pyrex refraction index, we see that the θ_{sci} angle of the light which is totally reflected inside the scintillator is 12^o.

The validity of these results is not limited to the simple situation examined here but is more general, as a complete computer simulation of the apparatus has shown.

The mentioned effects and the geometrical acceptance of the apparatus have been evaluated by a dedicated Montecarlo code. The simulation takes into account the radial distribution of the γ ray beam (which depends on the lead collimator geometry) and the absorption of the γ rays in the scintillator. Fig. 5 shows the radial distribution of the simulated events.

The main result is that the geometrical acceptance does not change substantially with the longitudinal position of the source. This is shown in a simulation where the effects due to the self-absorption of the scintillator are neglected. Figs. 6, 7, 8 show the results of these calculations. An energy deposit of 0.5 MeV was simulated (at 5 cm, 40 cm and 190 cm) assuming a scintillator yield of 10^4 photons/ MeV. Figs. 6a) 7a) 8a) show the number of photons reaching PMT1 as a function of the radius where the scintillation event was generated. Figs. 6b), 7b) 8b) are the corresponding histograms.

The distribution of the photons reaching PMT1 has a shape which changes by varying the source position but the mean number of the photons reaching PMT1 (and therefore the mean photoelectron number) is practically independent of the axial source position. This result is not related to the particular shape of the radial distribution of the events. In these conditions, if the experimental data show a decrease

of the number of detected photoelectrons versus the source position, this can only be due to the self-absorption of the light in the scintillator.

This last consideration is true for an ideal apparatus and specially for a Pyrex tube with perfect walls. In practice some light could be lost because the Pyrex tube is not an ideal cylinder or because its walls can have some impurity spots which absorbs some fraction of the light. These effects, if really present, give rise to an effective attenuation length which must be combined with that of the scintillator. The role played by these effects cannot be very substantial because of the small number of reflections made by the collected light on the Pyrex walls: for a light pathlength of 2 metres, a photon emitted on the axis makes no more than 4 reflections. Assuming a simple exponential light attenuation law, the measured attenuation length Λ will be related to the true attenuation length of the scintillator Λ_{sci} and to the "instrumental" attenuation $\Lambda_{instrum}$ by the simple law

$$\frac{1}{\Lambda} = \frac{1}{\Lambda_{sci}} + \frac{1}{\Lambda_{instrum}} \tag{4}$$

From the measurements of the attenuation length of scintillators having Cumene as solvent (see Sect. 5) we estimate that the effective attenuation length $\Lambda_{instrum}$ due to these spurious effects must be greater than 10 m. This possible systematic effect is not subtracted from the attenuation length reported in this paper.

The numerical calculations give for the geometrical efficiency ϵ the value

$$\epsilon \simeq 5 \ \ 10^{-3} \tag{5}$$

We repeat that this number is independent on the γ source position but its exact value depends on the real values of the refractive index of the air, of the scintillator and of the Pyrex in the wavelength region of our interest.

Assuming an absolute yield of $Y = 10^4$ photons/MeV, using (5), the expected number of photoelectrons detected by PMT1 without self-absorption is around 3-4.

2.2 Electronics

The electronics scheme (see Fig. 9) is such that for every event we measured:

- the charge of the signals of PMT1 and PMT2;

- the time difference of these two signals.

The data were acquired by a CAMAC system triggered by the coincidence between the two PMTs and the NaI counter. In order to reduce the background (coming for instance from cosmic rays) at the trigger level an energy deposition in the NaI counter of 220 ± 100 keV was required so that backscattered γ rays where selected.

3. CHOICE OF THE MIXTURES AND SCINTILLATOR HANDLING

Liquid organic scintillators are usually obtained by doping a solvent with an high concentration of a primary fluor and sometimes a much lower concentration of a secondary fluor [14]. The solvent can be itself a mixture of two or more components whose proportions are optimized in each specific experiment. The exceptional radiopurity required for the scintillator of the Borexino experiment sets tight limits on the choice of the scintillator formula. High light yield and low attenuation length must be obtained without using chemical components that cannot be purified at the required level. This excludes the possibility of using mixtures with mineral oil, for which the poor light output is compensated by the large tranparency [15], and discourages the use of a many components mixtures.

Measurements of the emission spectra and of the extinction coefficients made with a spectrophotometer using small sample of mixtures [16] have suggested the use of pseudocumene (1,2,4 trimethylbenzene) and cumene (isopropylbenzene) as solvents. These solvents are usually delivered with a purity of 99%.

PPO (2,5 -diphenyloxazole), PMP (1-Phenyl-3-Mesityl-2-Pyrazoline), have been selected as primary fluors and Bis MsB (p-bis(o-methylstyryl)benzene) as a secondary fluor. The nominal purity is 99%.

Before taking data the solvents were distilled by the Ismar Company [17]. The quality of the process has been controlled measuring the light absorption of a small volume (a few cubic centimeter contained in a cell of 10 cm of pathlength) of distilled liquid. For the same sample of solvent the distillation process has been repeated each time measuring the absorption. Usually after two processes, the absorption of the solvent reached its saturation value and a further distillation did not improve the transparency.

PPO was analysed to verify the presence of the most common metals having absorption spectra in the UV region. Such metals could be responsible for some degree of light attenuation. Table 1 summarizes the results of the analysis. Only Na and Ca have a concentration well above the resolution limit of the analyser. However their concentration are small enough to give a negligeable contribution to the optical properties of the scintillator.

During the preparation of the mixture special care has been devoted to remove the oxygen dissolved in the liquid. In fact, it is well known that oxygen acts as a light quencher [14]. For this reason, we fluxed nitrogen into the mixture: typically, about 10 litres of scintillator are fluxed with about 4000 liters of nitrogen gas. During the

filling operations the liquid remains in contact only with a nitrogen atmosphere and finally when the cell is closed it is left under nitrogen pressure.

Dust can in principle be present in the liquid solvent or in the solute and can absorbe or diffuse the light. We experimentally saw that dust removal was very effective for the PC+PMP mixtures (see the following). The cleanliness of every vessel containing the liquid sample was carefully controlled and a filtering system with two nylon 66 filters (with holes of 0.2 μm and 0.45 μm) was built. The mixture is prepared inside a stainless steel vessel, here the nitrogen flushing takes place and, from this vessel, the liquid fills the Pyrex cell of the counter after passing trough the two nylon filters.

4. CHARGE SPECTRA ANALYSIS

The study of the light self-absorption is accomplished by analyzing the mean number of photoelectrons versus the source position along the axis of the device. The knowledge of the signal corresponding to one photoelectron is necessary to perform the data analysis. With our photomultipliers this single photoelectron spectrum is easily obtained without any external source. In fact, due to the large photocathode area, the rate of emission of thermoionic electrons from the photocatode dominates that of the secondary dynodes: the result is that the dark current charge spectrum shows a clear single photolectron peak that allows the calibration of the photomultiplier. Fig. 10 shows the dark current charge spectrum of PMT1: the single photoelectron peak is clearly visible. A gaussian curve $f_{<Q_1>,\sigma_1}(q)$ having a mean value $< Q_1 >$ and standard deviation $< \sigma_1 >$ reproduce well the single photolectron response

$$f_{<Q_1>,\sigma_1}(q) = \frac{1}{\sqrt{2\pi}\sigma_1} exp^{-\frac{(q-<Q_1>)^2}{2\sigma_1^2}} \tag{6}$$

The response of the PMT to 2, 3,... n photoelectrons is still of gaussian form $f_{<Q_n>,\sigma_n}(q)$ having a mean value $< Q_n >= n < Q_1 >$ and a rms $\sigma_n = \sqrt{n}\sigma_1$.
The charge spectrum of the signals detected by one PMT when the scintillator is excited by the radioactive source is the superposition of signals corresponding to 1, 2, ...N photoelectrons. It can be described as

$$F(q) = A \sum_{k=1}^{N} P(k) f_{<Q_k>,\sigma_k}(q) \tag{7}$$

where A is a normalization constant and P(k) is the probability of having k photoelectrons. It is reasonable to assume that $P(k)$ is given by the Poisson law

$$P(k) =< n >^k exp^{-<n>}/k \tag{8}$$

where $< n >$ is the mean photoelectron number. This is the parameter of interest that must be obtained from each charge spectrum.

Fig. 11 shows a typical charge spectrum. This figure refers to a PC+PPO(1.5 g/l) mixture, the source was located 190 cm from the end of the Pyrex cell close to PMT1. Fig.12 is the distribution of the time difference of the signals reaching PMT1 and PMT2. A detailed analysis of the time response of our scintillators will be presented elsewhere.

The charge analysis has been performed by selecting the events whose timing differs from the peak of the distribution, like the one of Fig. 12, by less than 3 standard deviations. Background events coming from cosmic rays interacting in unknown positions inside the scintillator are thereby rejected.

For each source position, $< n >$ has been evaluated using two different methods. The first one consists in the fitting the charge spectra with the function of eq. (7). The parameters of the fits are $< n >$ and A.

The second method requires the calculation of the mean photoelectron number $< n_{exp} >$, as a ratio between the mean charge $< Q >$ of the measured spectra and $< Q_1 >$; the result has to be correcetd in order to account for the probability of detecting zero photoelectrons. Because of the small value of the number of detected photoelectrons, this correction is not negligeable.

In other words, the $< n_{exp} >$ value is first obtained by taking the ratio between the two measured quantities $< Q >$ and $< Q_1 >$

$$< n_{exp} >=< Q > / < Q_1 > \tag{9}$$

then the relation

$$< n_{exp} >= \frac{< n >}{1 - exp^{-<n>}} \tag{10}$$

is applied to get the $< n >$ value.

In principle the two methods of analysis should be equivalent and give the same result. In practice some difference is apparent due to the fact that the result of the last method is sensitive to the tails in the charge spectrum while the result of the fit is not; on the other hand, the fit method requires as input the shape of the single photoelectron response and its output depends on the parameteres of this curve, while the second requires only the knowledge of the mean value of the single photoelectron response. Taking into account all these considerations, the two methods of analysis gave results in good agreement.

5.SELF-ABSORPTION CHARACTERISTIC LENGTH: EXPERIMENTAL RESULTS

A self-absorption curve, that is a plot of $< n >$ versus the source position z, similar to the one of Fig. 13 was experimentally measured for all the mixtures investigated.

These curves show a fast initial decrease of the light yield and a second slower attenuation. To quantitatively describe these curves we fit them by a superposition of two exponential functions.

$$< n(z) >=< n_0 > [(1-r)\ \ exp(-z/\lambda) + r\ \ exp(-z/\Lambda)]\,, \qquad (11)$$

where

-z is the light pathlength;

- λ describes the initial fast light decrease;

- Λ characterizes the long distance light absorption and it is the most important parameter for CTF and Borexino;

- r could be identified with the fraction of the light which remains after the short distance absorption described by λ has taken place.

5.1 Results for Pseudocumene+PMP mixtures

PMP was added to Pseudocumene in two concentrations: 1.6 g/l and 2.5 g/l. The first measurements were made without filtering the mixtures. The values of λ and Λ do not change with the fluor concentrations (see Table 2). Then the mixture Pseudocumene+PMP(2.5g/l) was extracted from the Pyrex tube, filtered with the filtering apparatus and the counter was filled again. The attenuation length values were now larger, (the Λ value reaches 5 m) showing that the dust and the various impurities played a significant role in the light absorption process. The comparison of the filters used to filter the mentioned mixture and others used to filter only the solvent indicates that the largest fraction of the particulate comes from the fluor.

5.2 Results for Pseudocumene+PPO mixtures

Pseudocumene+PPO mixtures were investigated with PPO concentrations ranging from 1.5 g/l to 6 g/l. Data were taken with mixtures filtered and not filtered and, in this case, the results do not improve after the filtering process. We compared also mixtures made with the same PPO concentration and with solvent distilled once or twice, as described in Section 4. The results do not substantially change but we observe that mixtures made with solvents distilled twice gave Λ values more reproducible than the one obtained with solvent distilled only once. Table 3 summarizes some results about these mixtures.

5.3 Results for Pseudocumene+PPO+BisMsB mixtures

The Λ values obtained with the same mixtures with and without adding some BisMsb were compared. A given mixture of Pseudocumene and PPO was prepared, filtered and the self-absorption curve was measured. Then a small quantity of BisMsb was added, the mixture was filtered again and a new self-absorption curve was obtained. We have repeated this process various times, the remarkable result is that even a small concentration (see Table 3) of bisMsb, which shifts the emission spectrum toward longer wavelength values, has the effect of reducing the self-absorption of the mixtures giving Λ values of 3-4 metres.

5.4 Results for Cumene+PMP mixtures

The $\Lambda = 5$ m value found with PC+PMP is the maximum value measured using Pseudocumene. We investigated the possibility of getting a mixture with larger Λ value by choosing a different solvent. Some test has been performed using Cumene. As observed by coworkers [16] the mixtures Cumene/PPO are not stable: our data

have shown that the light yield halves in about 8 hours. The light emission of the mixture Cumune/PMP remains stable at level of the 1% for two weeks.

The attenuation length of Cumene+PMP (1.65 gr/l) has been measured. The Λ value found is the largest one we have measured: 10 ± 1 m (1σ). However a reduced light yield (compared with that of mixtures realized with Pseudocumene) was measured and some indications of chemical instability was observed.

5.5 Results for PC + PPO + Bis-MSB + water mixtures

Due to the special feature of CTF and BOREXINO, we have carefully studied the effect on the light yield and on the attenuation length of water dissolved in the scintillator. The permeability of the nylon bag containing the scintillator to the water is not low enough to prevent small amounts of water infiltrating from the tank into the scintillator. Due to the low solubility of the water in PC, two distinct liquid phases should be produced at concentrations Water/PC higher than few hundred ppm's. We found that, at a temperature of 25 ^oC, for concentration Water/PC greater than about 300 ppm, the aqueous phase appears and the solution becomes opaque. The aqueous phase slowly deposits on the surfaces of the vessel. Owing to the low transparency, the resulting scintillator mixture is unsuitable for detector use. Instead, for concentration water/PC lower than 275 ppm at 25 ^oC, the mixture is clear.

To characterize the water/PC mixture we performed two set of measurements: 1) relative yield as function of water content, 2) attenuation length at water/PC concentration below the saturation value using the apparatus described above.

The measurement of the yield of a PC/PPO/Bis-MSB/water mixture was executed in a small bottle (100 ml approx.) of pyrex covered by aluminized-mylar

and optically coupled to a small PMT. A Bi^{207} gamma ray and electron internal conversion source was used to irradiate the mixture. The source was placed over the free surface of the scintillator and protected by a thin alumined-mylar foil. In the detected spectra the most prominent peaks are at 1.05 MeV (electron line) and at 0.7 MeV (Compton edge of the 1.05 MeV gamma ray line). As a relative yield measurement was taken the centroid of the Compton peak at 0.7 MeV. This peak has been monitored for several days and at with several water/PC concentrations. The data show a 0.6% reduction of the yield for concentration water/PC ranging from 0 to 1000 ppm. This small reduction of yield happens between 300 and 400 ppm.

The results of the measurements with the 2 m Pyrex cell indicate that the short and the long attenuation length do not change, within the measurement errors, when the concentration water/PC is lower than the saturation value for the PC/PPO/Bis-MSB mixture with 175 and 275 ppm of water.

We conclude that for a PC/PPO/Bis-MSB mixture the presence of water at concentration below the saturation value at 25 ^oC does not degrade the scintillator performances.

6. LIGHT YIELD

Our extimation of the light yield relies on the analysis of the mean photoelectron number detected by PMT1 when the source is located 5 cm far from the end of the Pyrex cell. The comparison of the data about Pseudocumene/PPO with the solvent distilled only once and that obtained with Pseudocumene distilled twice, shows that the double distillation process gives a mixture with an yield larger than the previous one by about 20%. Within an error of 10%, the ligth yield of the PC+PMP mixtures

is equal to the one of the double distilled samples of PC+PPO. The presence of BisMsB does not change appreciably the ligth output of the mixture.

The absolute light yield is not easily evaluated because of the uncertainty in the knowledge of some parameters (e.g. photocathode quantum efficiency, single photoelectron counting efficiency etc.). Our results are compatible with an absolute light yield of the order of $1 - 1.2 \ 10^4 \ \gamma$ /MeV.

7.INTERPRETATION OF THE RESULTS AND CONCLUSIONS

In an ideal scintillator which does not contain impurities of any type, the light attenuation is due to the superposition between the emission spectrum and the absorption spectrum of the solute and of the solvent. This superposition is not complete because the emission spectrum is usually shifted in a region of longer photon wavelength than the absorption spectrum. The mixtures theoretically more transparent are those having the largest shift (Stokes shift). Our results on the Λ values measured for Pseudocumene+PMP,Pseudocumene+PPO, Pseudocumene+PPO+BisMsb agree with this hypothesis: we have found larger Λ values for Pseudocumene+PMP, whose emission spectrum peaks around 425 nm, than for Pseudocumene+PPO, which has an emission spectrum reaching its maximun around 360-370 nm [16]. The increasing of Λ after adding the BisMsb to the Pseudocumene+PPO mixtures is also explained by the same argument: BisMsB has an emission spectrum shifted in a region of larger wavelength values than Pseudocumene+PPO [16].

The absorption of light by the solvent seems to be the most important process that determines the long distance attenuation length Λ because of the soft dependance of the Λ value on the fluor concentration. Published values on the attenuation length of Pseudocumene [13], obtained with a photometer and with light pathlength

comparable with that of our apparatus, agree with our best results. The fluctuations from sample to sample could be related to the presence of impurities.

The shape of the self-absorption curves arises from the superposition of the different attenuation length of the photons of various energies: a simple exponential light attenuation is in fact expected for monochromatic light [14]. The presence of an extended light emission spectrum results in a complex light self-absorption curve. The fit with two exponentials has not a real physical meaning but it is a useful description of the results. We think that the fast light attenuation, described by λ, could be interpreted as the result of the absorption of the photons which have energy in the region where the absorption spectrum is maximum, while the Λ value would be related to the absorption of the photons of lower energy for which the absorption is smaller.

The superposition between the emission and the absorption spectra suggests that the absorbed photons could be reemitted. Some data indicating the existence of this process can be found in the literature [18]. If a photon with energy E is absorbed there is a probability that another photon could be reemitted with energy $E' < E$. This photon can be itself absorbed and eventually a further photon with energy $E'' < E'$ could be reemitted originating a cascade process that stops when the energy of the photons is to low and lies in a region where there is no more superposition between the absorption and emission spectra. The reemitted photons will be uniformly distribuited over the entire solid angle and, using a cylindrical detector, which selects the light emitted into a small fraction of the solid angle, the most part of the reemitted light is lost. A 4π detector, like CTF or Borexino, will in principle detect all the reemitted light. If this process is real when a scintillation event is generated in the center of the spherical scintillator bag of CTF or Borexino,

the light intensity reaching the surface of the sphere will be larger than that obtained using relation (13) with z equal to the sphere radius. The disavantage is that some loss of position resolution could result.

At the moment there are not data available to clearly identify the existence of this process or to extimate its importance. The construction of a complete theoretical model introduces many parameters whose values are not easily obtainable from experiments (for instance the probability of reemission at any order) and it is a diffucult task. A simple model where the emission spectrum consists only of N_1 photons with energy E_1 and attenuation lenght Λ_1, and N_2 with energy E_2 and attenuation lenght Λ_2, could help to understand some features of the process. Using this simple model it easily found that the amount of the reemitted light, which is collected in a cylindrical apparatus, has to increase almost linearly with the radius a of the apparatus. This result is confirmed by the fact that some measurements of the attenuation length of PC+PPO and PC+PMP mixtures undertaken in a cylindrical cell having a smaller diameter than our cell, gave an attenuation curve similar to Fig. (13) but with a smaller r values and a faster initial light decrease [19]. Further investigations are necessary; however we believe that the final answer about the contribution of the reemitted light will come from the comparison of attenuation measurement done with the same mixtures in a cylindrical detector and in a spherical one like CTF.

As a summary we can say that the results of this work indicate that a scintillator with the optical property necessary for CTF can be obtained using Pseudocumene as solvent. Pseudocumene+PPO offers some advantage with respect to Pseudocumene + PMP from the timing point of view [20] and has been selected for the first run of CTF. Looking toward Borexino, mixtures having a Λ value of the order of 6 m or

better are to be preferred: good candidates are Pseudocumene+PMP or mixtures realized with Cumene as solvent. Further investigations are in progress.

REFERENCES

[1] C. Arpesella et al. (Borexino Coll.)

"Borexino at G. Sasso:proposal for a real time detector for low energy solar neutrinos" (1991);

Borexino Coll. "Borexino: a real tine detector for low energy solar neutrinos" Proposal submitted to the Nat. Sci. Found.

[2] M. Giammarchi on behalf of the Borexino Coll., Nucl. Phys. B (Proc. Suppl) 35 (1994) 433

[3]a) J. N. Bahcall, R. Ulrich, Rev. Mod. Phys. 60 (1988) 297

b) J. N. Bahcall, M. H. Pinsonneault, Rev. Mod. Phys. 64 (1992) 885

[4] R. Davis jr., Workshop on neutrinos telescope, Ed. by M. Baldo Ceolin, Venice (Italy) (1990) pag. 1

[5] P. Anselmann et al., Phys. Lett. B314 (1993) 445

[6] K. S. Hirata et al., Phys. Rev. Lett. 65 (1990) 1297

[7] V. N. Gavrin et al., Nucl. Phys. B (Proc. Suppl.) 35 (1994) 412

[8] SNO Coll., Phys. Lett. B 194 (1987) 321

[9] G. Bonvicini, Nucl. Phys. B (Proc. Suppl.) 35 (1994) 438

[10] P. Cennini et al. (ICARUS coll.) "ICARUS II: a second generation prton decay experiment and neutrino observatory at the G. sasso Laboratory" LNGS-94/99-I (1994)

[11] Y. Suzuki, Nucl. Phys. B (Proc. Suppl.) 35 (1994) 273

[12] Landolt-Bornestein, "Numerical data and functional relationship in science and technology" Vol.3 (1967)

[13] K. Eitel et al., Nucl. Instrum. and methods in phys. res. A 340 (1994) 346

[14] J. B. Birks, "The theory and practic of scintillation counting" (1964) Pergamon Press

[15] Macro Coll., Nucl. Instrum. and Meth. in Phys. Res. A324 (1993) 337

[16] F. Masetti et al. -Chem. Dep. of the Univ of Perugia (Italy)- (private communications)

[17] ISMAR chimica, Via Isocorte 16 ,16146 Genova (Italy)

[18] J.M. Martinho et al.,J. Chem Phys. 90 (1989) 53

[19] S. Schoenert et al. -Tech. Univ. Munich; Garching Germany- (private communication)

[20] G. Ranucci et. al. to be published on Nucl. Instrum and Methods in Phys. Res.

FIGURE CAPTIONS

Figure 1 - Experimental setup.

Figure 2 - Response of the apparatus as a function of the light wavelenght. The PMT quantum efficiency and the transmission of Pyrex window are shown.

Figure 3 - Cross section of the apparatus of Fig 1. showing the source collimator and the NaI counter.

Figure 4 - Details of the apparatus shown in Fig. 1

Figure 5 - Radial distribution of the point sized scintillation events generated by the Montecarlo code. The results about the geometrical efficiency are practically unchanged by using a uniform distribution of events.

Figure 6,7,8 - Number of photoelectrons detected by PMT1 when the source is placed at different positions along the tube axis (5 cm, 40 cm and 190 cm) and related histograms. While the shape of the distributions is position dependent, its mean value varies very little. The geometrical efficiency is practically position independent.

Figure 9 - Scheme of the electronics.

Figure 10 - Dark current spectrum of PMT1 showing the single photoelectron peak.

Figure 11 - Charge spectrum of the signals detected by PMT1 when the source position is z=5cm. The mixtures here is PC +PPO (1.5 g/l). The result of the fit with function (7) is superimposed. P1 is the mean photoelectron number, P2 is a normalization.

Figure 12 - Typical time difference distribution. The peak structure (FWHM=5.7 ns) allows the selection of the events generated by the source or, in any case, localized

around the source position. The detailed analysis of the time distribution spectra will be presented elsewhere.

Figure 13 - Typical plot of the mean photoelectron number versus the source position. A curve of this shape is obtained for all the mixtures.

Figure 14 - Self absorption curve of PC+PMP (2.5 g/l) with and without filtering. The upper curve refers to the mixture not filtered. The lower one to the same mixture filterd as described in the text.

TABLE 1

Metals in PPO

Element	*Concentration (ppm)*
Zn	< 0.40
Cd	< 0.03
Sr	< 0.11
Pb	< 0.45
Bi	< 0.36
Co	< 0.08
Ni	< 0.16
Ba	< 0.05
Fe	< 0.10
Mn	< 0.02
Cr	< 0.08
Mg	< 0.01
Be	< 0.01
Cu	< 0.06
Ag	< 0.08
Ca	3.84
K	< 0.10
Na	9.66

TABLE 2

PC/PMP

$PMP\ (gr/l)$	$filter$	$\lambda\ (cm)$	$\Lambda\ (m)$	r
1.6	*no*	15 ± 1	1.9 ± 0.2	0.7
2.5	*no*	21 ± 2	1.9 ± 0.2	0.7
2.5	*yes*	43 ± 10	5.0 ± 0.5	0.64

TABLE 3

PC/PPO/Bis-MsB

$PPO\ (gr/l)$	$Bis-MsB\ (gr/l)$	$filter$	$\lambda\ (cm)$	$\Lambda\ (m)$	r
5.5	–	*yes*	10 ± 3	1.8 ± 0.2	0.6
2.5	–	*yes*	28 ± 3	2.7 ± 0.4	0.7
1.5	–	*yes*	11 ± 4	2.0 ± 0.3	0.52
1.5	0.02	*yes*	22 ± 5	3.6 ± 0.3	0.7
1.5	0.05	*yes*	20 ± 6	3.1 ± 0.3	0.64
1.	–	*yes*	15 ± 2	1.5 ± 0.1	0.6
1.	0.2	*yes*	20 ± 3	3.0 ± 0.4	0.6

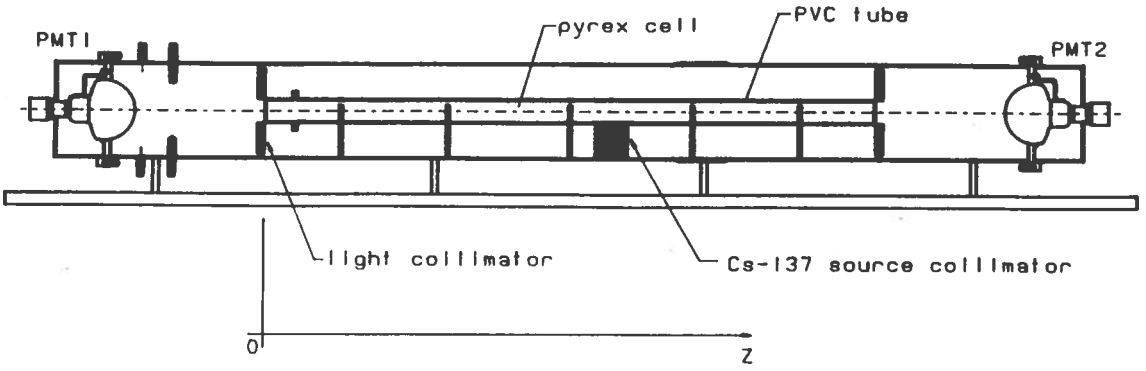
PMT1
pyrex cell
PVC tube
PMT2
light collimator
Cs-137 source collimator
0
Z

Fig. 1

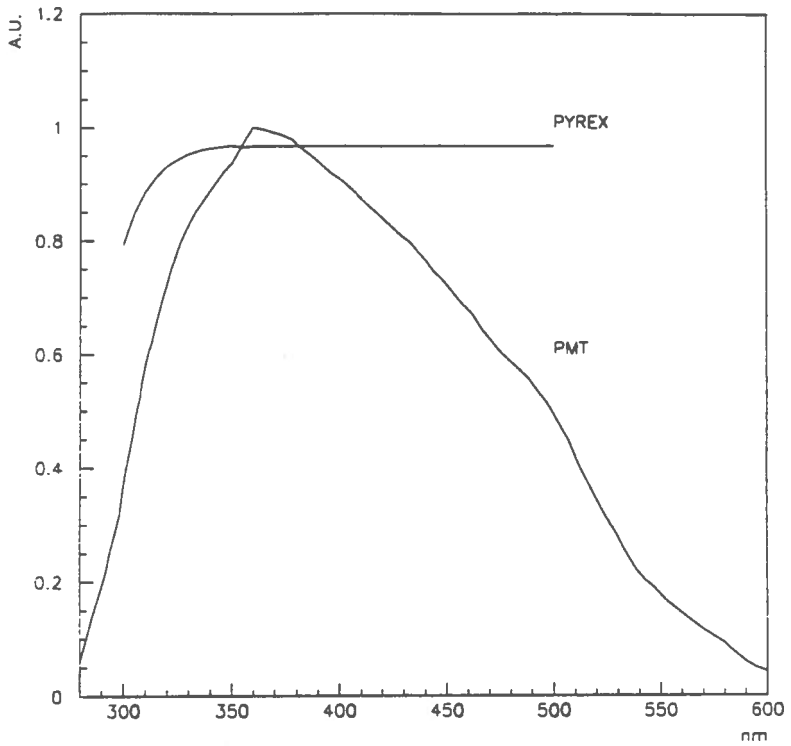
A.U.
1.2
1
0.8
0.6
0.4
0.2
0
PYREX
PMT
300
350
400
450
500
550
600
nm

Fig. 2

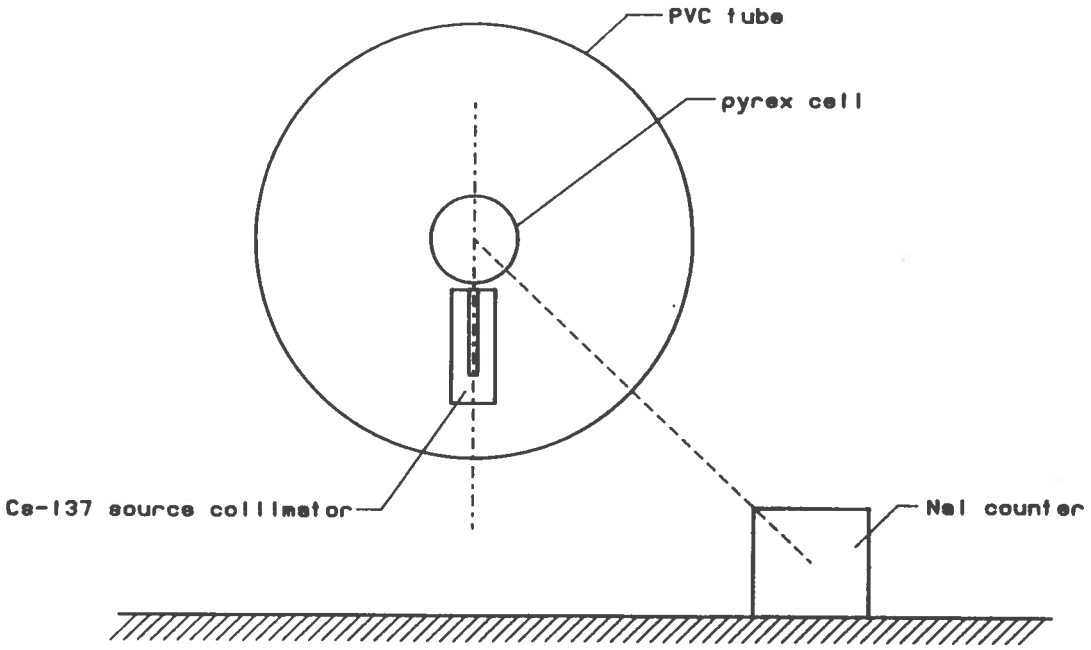
PVC tube
pyrex cell
Cs-137 source collimator
NaI counter

Fig. 3

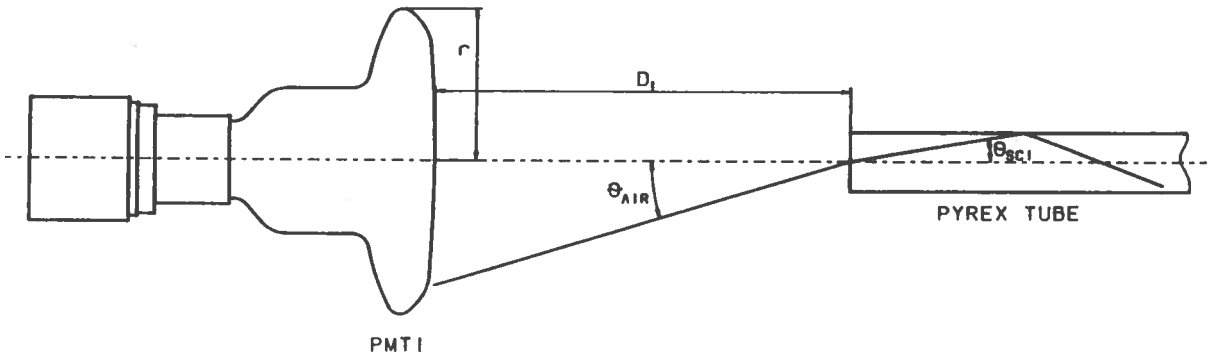
r
D_t
θ_{AIR}
θ_{SCI}
PYREX TUBE
PMTI

Fig. 4

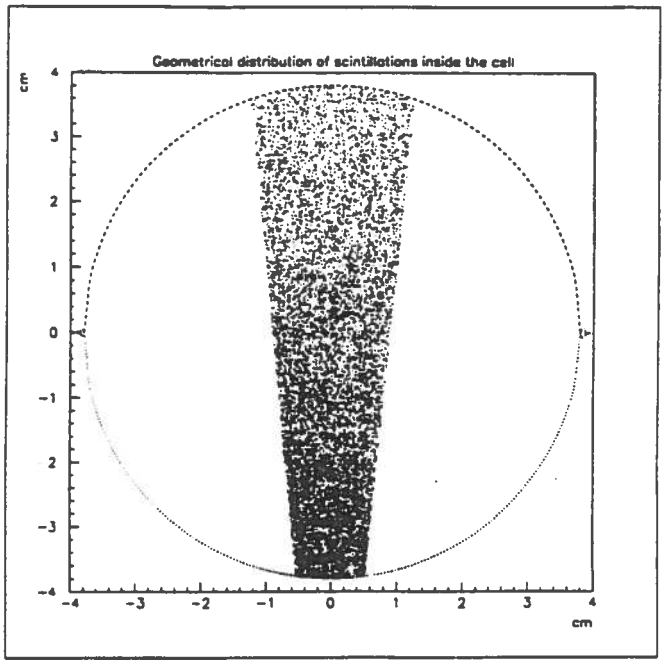
Geometrical distribution of scintillations inside the cell
cm
cm

Fig. 5

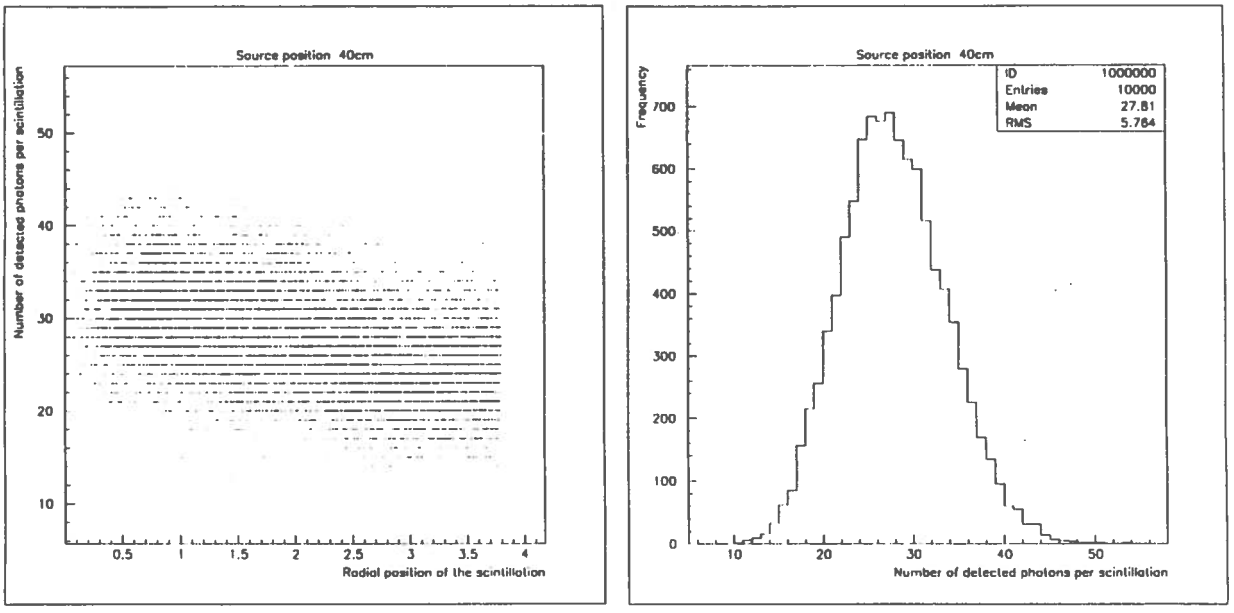
Source position 40cm
Number of detected photons per scintillation
Radial position of the scintillation
Source position 40cm
Frequency
ID 1000000
Entries 10000
Mean 27.81
RMS 5.784
Number of detected photons per scintillation

a) **b)**

Fig. 6

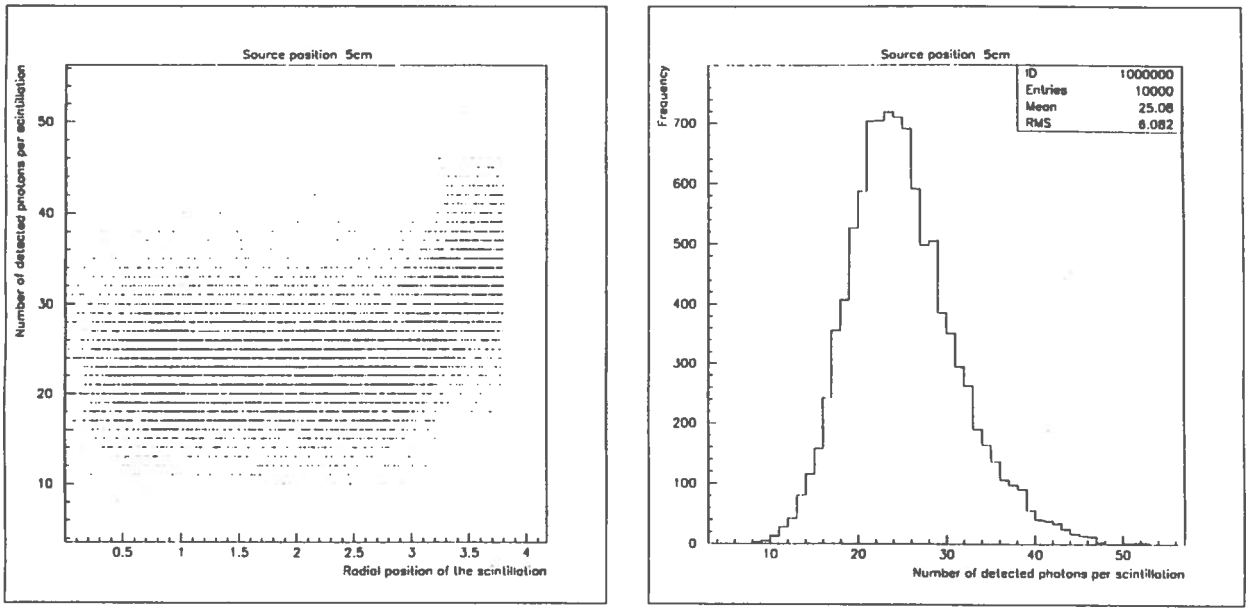

a) b)

Fig. 7

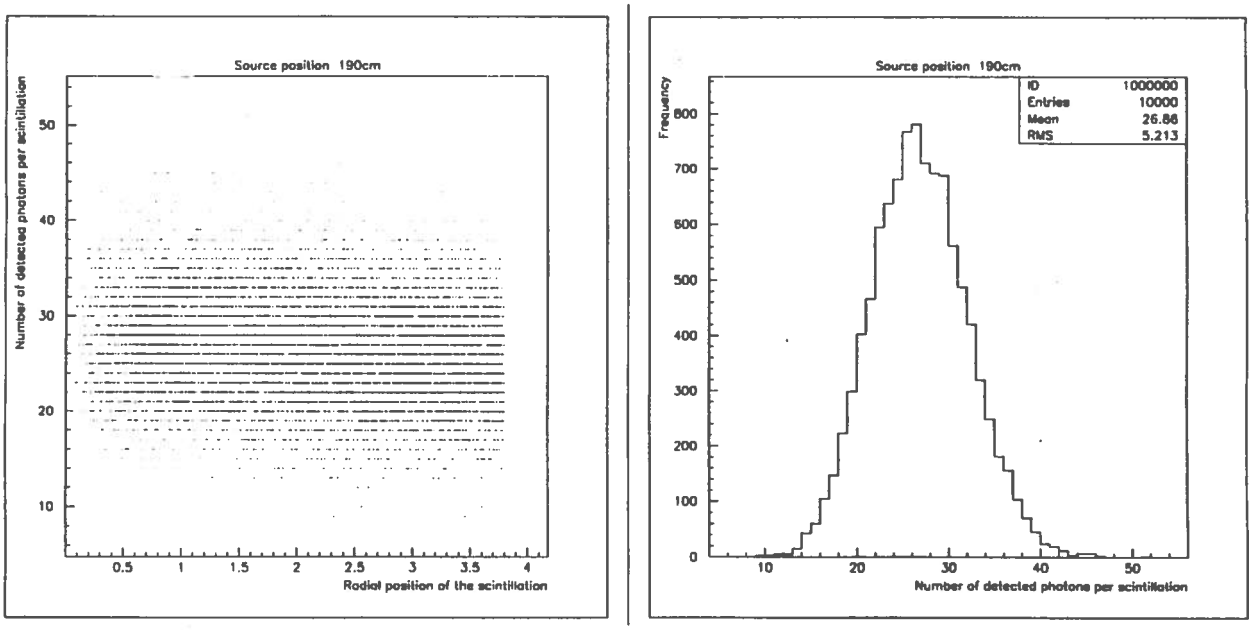

a) b)

Fig. 8

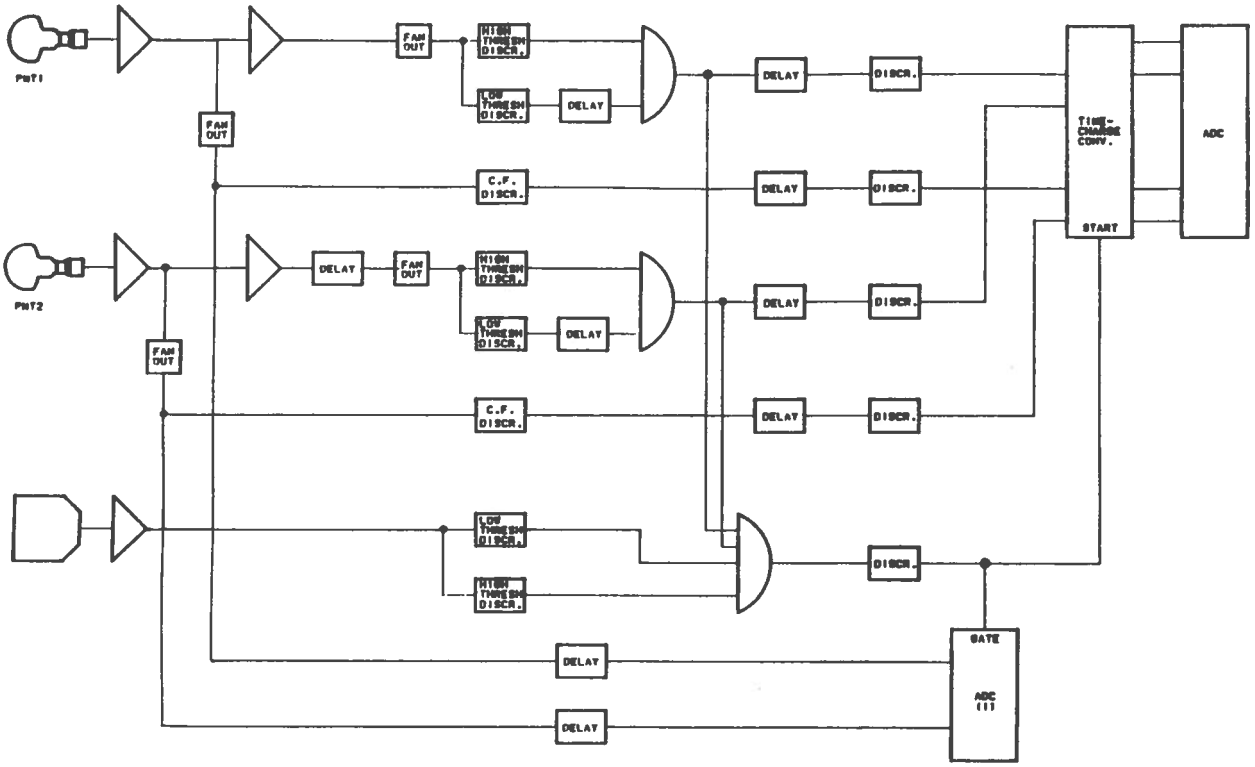
PMT1
PMT2
FAN OUT
HIGH THRESH DISCR.
LOW THRESH DISCR.
DELAY
C.F. DISCR.
DISCR.
TIME-CHARGE CONV.
START
ADC
GATE
ADC 111

Fig. 9

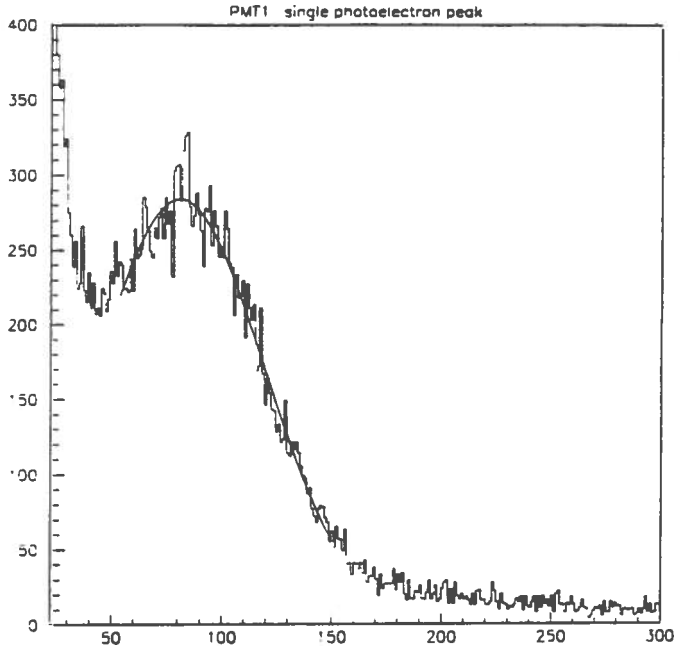
PMT1 single photoelectron peak
400
350
300
250
200
150
100
50
0
50
100
150
200
250
300

Fig. 10

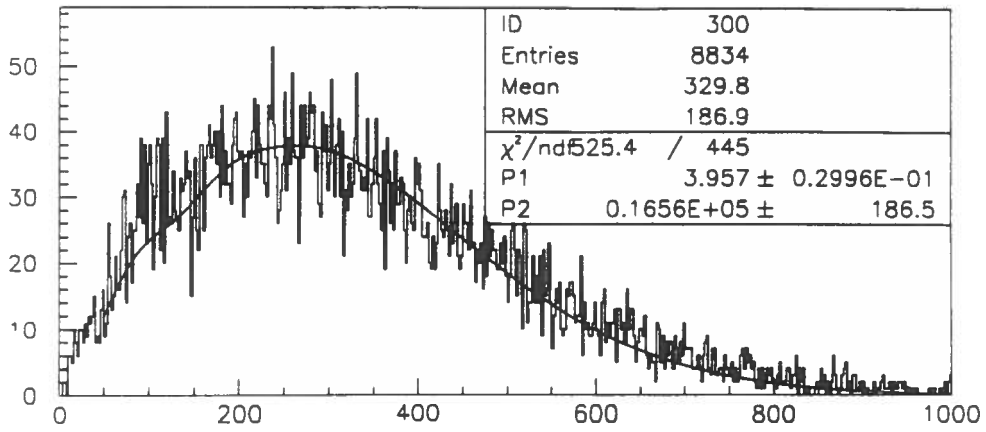
ID 300
Entries 8834
Mean 329.8
RMS 186.9
χ²/nd 525.4 / 445
P1 3.957 ± 0.2996E-01
P2 0.1656E+05 ± 186.5
0
10
20
30
40
50
0
200
400
600
800
1000

Fig. 11

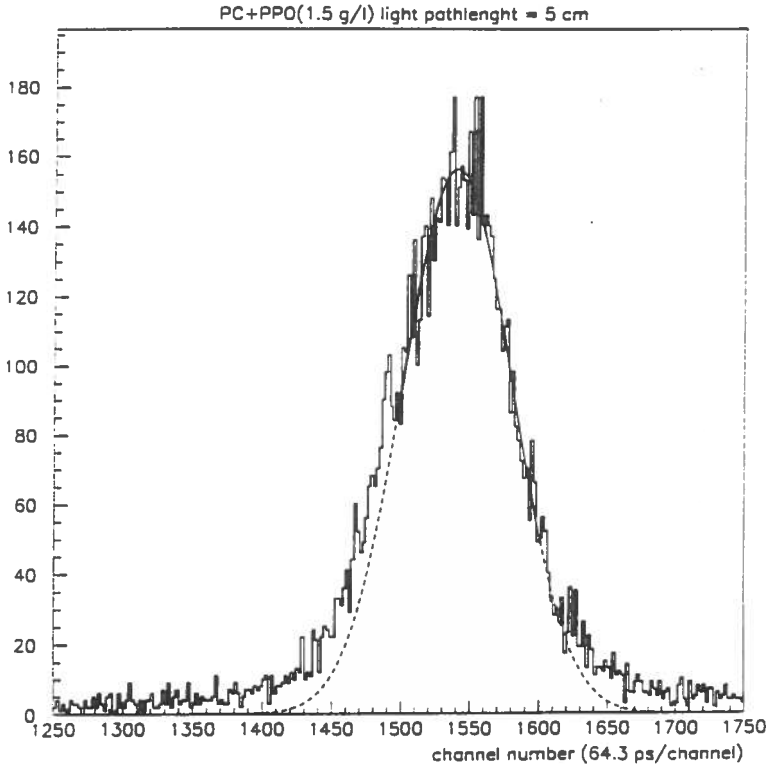
PC+PPO(1.5 g/l) light pathlenght = 5 cm
0
20
40
60
80
100
120
140
160
180
1250
1300
1350
1400
1450
1500
1550
1600
1650
1700
1750
channel number (64.3 ps/channel)

Fig. 12

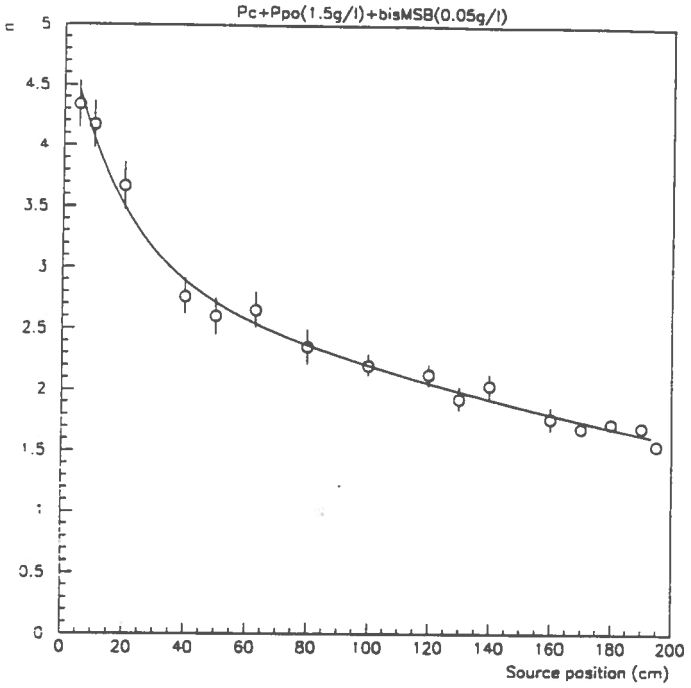
Pc+Ppo(1.5g/l)+bisMSB(0.05g/l)
Source position (cm)

Fig. 13

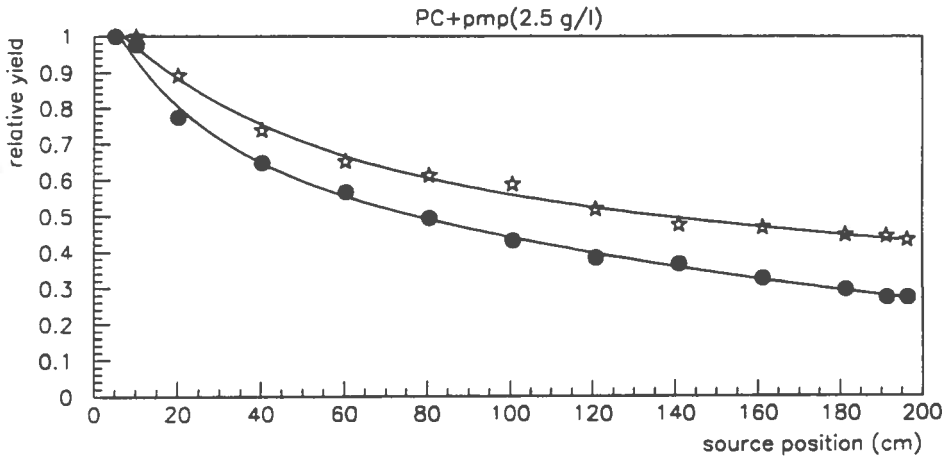
PC+pmp(2.5 g/l)
relative yield
source position (cm)

Fig. 14